Astron. Astrophys. 314, 503–513 (1996)

ASTRONOMY AND ASTROPHYSICS

Distribution of starspots on cool stars

I. Young and main sequence stars of 1 $M_\odot$

M. Schüssler[1], P. Caligari[1], A. Ferriz-Mas[2], S.K. Solanki[3], and M. Stix[1]

[1] Kiepenheuer-Institut für Sonnenphysik, Schöneckstr. 6, D-79104 Freiburg, Germany
[2] Instituto de Astrofisica de Canarias, E-38200 La Laguna (Tenerife), Spain
[3] Institut für Astronomie, ETH-Zentrum, CH-8092 Zürich, Switzerland

Received 26 October 1995 / Accepted 17 March 1996

Abstract. Sunspots are restricted to a latitude band within 30° of the solar equator. In contrast, the latitudes of spots on the surfaces of rapidly rotating cool stars can range from their polar regions, for RS CVn systems and for T Tauri stars leaving the Hayashi track, to mid latitudes for stars close to or on the main sequence. In order to find an explanation for these observed spot latitudes we have applied the criteria for the undulatory instability (Parker instability) of a toroidal magnetic flux tube embedded in the convective overshoot layer below the outer convection zone and calculated the non-linear evolution of the rising magnetic loops formed by this instability. We describe the results for a star of one solar mass in different phases of its evolution before and on the main sequence. We find that there usually is a range of latitudes at which magnetic flux can emerge on the stellar surface. The mean latitude of emergence shifts towards the poles for increasingly rapid rotation. The internal structure of the star, however, plays an almost equally important role in determining the latitude of magnetic emergence. For stars of solar mass only the youngest objects, with extremely deep convection zones, should show spots emerging at the stellar poles. Pre-main sequence stars at an age of 10^7 y (convection zone reaching down half-way to the centre) exhibit high latitude, but not truly polar spots, while a main sequence star of one solar mass, even at high rotation rates, only shows intermediate latitude spots. These results are found to be in good agreement with Doppler images of young rapid rotators.

Key words: stars: magnetic fields – stars: activity – MHD

1. Introduction

The last decades have seen the introduction (Vogt and Penrod 1983) and widespread use of Doppler imaging techniques which allow the surface patterns of rapidly rotating stars to be reconstructed. The resulting images have strikingly confirmed the presence of large, dark starspots, whose existence had long been suspected from photometric time series. Zeeman and magnetic Doppler imaging by Donati et al. (1992) and Saar et al. (1994) suggest that starspots are associated with magnetic fields.

The major surprise provided by Doppler imaging has been the high latitudes of many (but not all) of the starspots, with a sizable fraction of the imaged stars actually showing dark polar caps. This result is in striking contrast to the case of the Sun, for which spots are observed exclusively at low latitudes. An explanation for the high latitudes of starspots on rapid rotators has been proposed by Schüssler and Solanki (1992), who pointed out that the Coriolis force (arising from angular momentum conservation) deflects magnetic flux tubes rising through the stellar convection zone towards higher stellar latitudes. Since the Coriolis force increases with decreasing rotation period, $P_{\rm rot}$, it becomes dominant for rapidly rotating stars. Such stars are therefore expected to show high latitude activity.

In the last years there has been considerable progress in this kind of observations. The number of Doppler imaged stars has increased considerably, so that it has become possible to distinguish between, on the one hand, young pre-main sequence and main sequence stars (e.g., T Tauri stars, BY Draconis stars) and, on the other hand, more evolved objects (like RS CVn binaries and FK Comae stars).

The observations suggest that most of the rapidly rotating giants and subgiants have spots concentrated strongly towards high latitudes and even completely covering the visible poles (e.g. HR 1099, $P_{\rm rot}$ = 2.8d, Vogt 1988; Donati et al. 1992; UX Ari, $P_{\rm rot}$ = 6.4d, Vogt & Hatzes 1991; HD 26337, $P_{\rm rot}$ = 1.9d, Strassmeier et al. 1991; Hatzes & Vogt 1992; HD199178, $P_{\rm rot}$ = 3.3d, Vogt 1988; HU Vir, $P_{\rm rot}$ = 10.3d, Strassmeier 1994).

The situation is more complex for younger stars, which show a whole range of spot latitudes even in the case of very rapid rotators. For example, the weak-line T Tauri star HDE 283572 ($P_{\rm rot}$ = 1.55d) shows a complete polar cap (Joncour et al. 1994b), while another weak-line T Tauri star, V410 Tau ($P_{\rm rot}$ = 1.87d), exhibits mainly high latitude starspots reaching up to the pole, but no complete polar cap (Joncour et al. 1994a,

Send offprint requests to: M. Schüssler

Strassmeier et al. 1994, Hatzes 1995). HD 155555, the primary of a post-T Tauri binary ($P_{\rm rot}$ = 1.68d), shows both high- and mid-latitude spots (Kürster et al. 1992) while LQ Hya, a single BY-Dra type star ($P_{\rm rot}$ = 1.60d), has high latitude, almost polar features, but also many low-latitude spots (Saar et al. 1994; Strassmeier 1990). Finally, the single pre-main sequence star AB Dor ($P_{\rm rot}$ = 0.51d) shows an active band between 15 and 35 degrees from the equator, but still considerable spottedness at higher latitudes, right up to the pole according to Kürster et al. (1992, 1994). Collier Cameron & Unruh (1994) and Unruh et al. (1995), on the other hand, find the high-latitude band between 50° and 80° to be heavily spotted, with an additional low-latitude band of spots. All the above stars have rotation periods of less than 2 days and certainly qualify as rapid rotators ($\Omega \approx 15$–$60\,\Omega_\odot$), but show very different latitude dependences of their spots, ranging from only a polar cap (HDE 283572) to enhanced spottedness in a relatively low latitude band (AB Dor).

In the present paper we present a first attempt to understand this range of spot latitudes in young stars. The current thinking is that the magnetic fields of active cool stars are generated by a dynamo residing in the overshoot layer at the bottom of the stellar convective envelope. The dynamo produces strands of toroidal field which, once the field strength exceeds a critical value, become subject to non-axisymmetric instabilities. This leads to the development of loop structures, which rise through the convection zone, erupt at the surface, and form active regions and magnetic spots (e.g., Schüssler et al. 1994). The path through the convection zone is determined by the buoyancy force, acting radially outwards, the Coriolis force, which is perpendicular to the axis of rotation, together with the magnetic tension and drag forces. The relative strengths of these forces depend on a variety of parameters, but mainly on the angular rotation rate and on the magnetic field strength. The latter in turn depends on the stellar structure, in particular on that of the overshoot layer below the convection zone, the latitude and the stellar (differential) rotation.

We consider an evolutionary sequence of stellar models of $1M_\odot$ from the Hayashi track onto the main sequence. For rotation rates between $1\,\Omega_\odot$ and $60\,\Omega_\odot$, where $\Omega_\odot = 2.7 \cdot 10^{-6}\ {\rm s}^{-1}$ is the (equatorial) rotation rate of the Sun, we determine the stability properties of toroidal flux tubes using results from a linear stability analysis (Ferriz-Mas and Schüssler 1993, 1994, 1995). We follow the nonlinear evolution of the undulatory instability (Parker instability) of flux tubes and determine the latitude of magnetic flux emergence by numerical calculation of the trajectory of rising flux tubes on the basis of the 'thin flux tube approximation' (Spruit 1981) of the MHD equations. The combined approach of linear stability analysis and nonlinear simulation has been previously applied to the Sun and successfully used to explain the observed emergence latitudes, tilts, proper motions and asymmetries of active regions (Moreno-Insertis et al. 1994a,b; Schüssler et al. 1994; Caligari et al. 1995).

2. Equilibrium and stability of magnetic flux tubes

The well-observed properties of sunspot groups (e.g., Zwaan & Harvey 1994) indicate that they originate from a coherent magnetic structure, which emerges from a source region of well-ordered, toroidal magnetic flux in the solar interior. As a working hypothesis, we assume that the same basic processes as in the solar case operate also in magnetically active stars with outer convection zones. The coherent magnetic structures are described as *magnetic flux tubes*, i.e., bundles of magnetic field lines that are separated from their non-magnetic environment by a tangential discontinuity with a surface current. As a consequence, the coupling between the flux tube and its environment is of a purely hydrodynamic nature, mediated by pressure forces, so that the tube can move even through a perfectly conducting plasma. Possible formation processes for flux tubes are *flux expulsion* by convective flows (Proctor & Weiss 1982) and the magnetic Rayleigh-Taylor instability (Cattaneo & Hughes 1988).

It is improbable that the toroidal magnetic flux system generated by the dynamo is stored within the superadiabatically stratified convection zone of a cool star. Magnetic buoyancy (Parker 1975) and convective instability (Spruit & van Ballegooijen 1982) lead to loss of magnetic flux from the convection zone on a time scale of months, leaving insufficient time for convection and differential rotation to build up the field in the dynamo cycle. A more plausible site for generation and storage of magnetic flux is the region of convective overshoot below the convection zone proper (e.g., Spiegel & Weiss 1980): while the stratification is stable and allows magnetic flux tubes to attain a state of mechanical equilibrium, turbulence and flows are available for the working of the dynamo.

Equilibrium configurations of toroidal flux tubes (flux rings) situated in planes parallel to the stellar equator (i.e., at constant latitude) have been studied by Moreno-Insertis et al. (1992). The star is assumed to be in stationary equilibrium and large-scale flows are neglected except for (differential) rotation. The force equilibrium perpendicular to the axis of the flux tube is then determined by a balance of buoyancy force, magnetic curvature force, and rotationally induced (centrifugal and Coriolis) forces. Since the curvature force and the rotational forces are perpendicular to the axis of rotation, the component of the (radial) buoyancy force parallel to the axis cannot be balanced. Hence, except for flux tubes located *exactly* within the equatorial plane, the buoyancy force must vanish in equilibrium, i.e., the density within the flux tube must be equal to the density in its exterior. The equilibrium is then determined by a balance of the magnetic curvature and rotational forces, leading to the condition

$$R_0^2(\Omega^2 - \Omega_{\rm e}^2) = v_{\rm A}^2\,, \qquad (1)$$

where Ω and $\Omega_{\rm e}$ are the angular velocities of the matter within the flux tube and in its environment, respectively; R_0 is the distance of the flux tube to the axis of rotation, and $v_{\rm A} = B_0/\sqrt{4\pi\rho_0}$ is the Alfvén speed in the tube (B_0: magnetic field strength, ρ_0: density in the tube). Moreno-Insertis et al. (1992) discuss how

Table 1. Properties of the stellar models used in this paper. The given quantities are the age, the radius in units of the present solar radius ($R/R_\odot$), the luminosity in units of the present solar value ($L/L_\odot$), the effective temperature ($T_{\rm eff}$), the radial position of the bottom of the overshoot region (r_0) and its fractional radius (r_0/R), the thickness of the overshoot layer (d), also as a fraction of the local pressure scale height (d/H), and the superadiabaticity $\delta \equiv \nabla - \nabla_{\rm ad}$ near the bottom of the overshoot layer. The values for model T marked with an asterisk (*) have been estimated following Zahn (1991).

Model	Age (yr)	$R/R_\odot$	$L/L_\odot$	$T_{\rm eff}$ (K)	r_0 (Mm)	r_0/R	d (Mm)	d/H	δ
M	$4.64 \cdot 10^9$	1.	1.	5780	504.	0.72	8.1	0.15	$-2.61 \cdot 10^{-6}$
P	$1.06 \cdot 10^7$	1.18	0.47	4400	441.	0.54	22.4	0.2	$-5.77 \cdot 10^{-7}$
T	$2.08 \cdot 10^6$	1.93	1.17	4333	211.*	0.16*	117.*	0.3*	$-2.92 \cdot 10^{-8(*)}$

such a state of mechanical equilibrium with $\Omega > \Omega_e$ and $\rho_0 = \rho_e$ (ρ_e: density outside the tube) is actually attained.

If magnetic flux is stored in mechanical equilibrium in a stably stratified overshoot layer, the question arises as to how it may eventually erupt and form active regions at the surface. It turns out that the equilibrium becomes unstable once a critical magnetic field strength is exceeded (Spruit & van Ballegooijen 1982): non-axisymmetric perturbations allow a downflow of plasma along the magnetic field lines from the summits towards the valleys of an undulatory perturbation. This increases the buoyancy of the summit regions, which continue to rise while the valleys sink. The result is a rapidly rising flux loop, which eventually breaks through the surface and forms a bipolar magnetic region while the footpoints become firmly anchored in (or below) the overshoot region (Moreno-Insertis 1986).

Ferriz-Mas & Schüssler (1993, 1995) have carried out a general linear stability analysis for equilibrium configurations of toroidal flux tubes according to Eq. (1), including the effects of stratification and (differential) rotation. The resulting dispersion relation is a sixth-order polynomial with real coefficients. Its roots represent six wave modes, which are related to the longitudinal and transversal tube waves. The nature of these modes in the special case of a toroidal tube in the equatorial plane of a star has been discussed by Ferriz-Mas & Schüssler (1994).

In the case of the Sun the linear stability analysis predicts that flux tubes stored in the overshoot region become first unstable in middle and low latitudes if their field strength exceeds about 10^5 G. This threshold for undulatory instability coincides with the value for the initial field strength required for low-latitude eruption of flux loops and a number of other observed properties of solar active regions (Choudhuri & Gilman 1987, d'Silva & Choudhuri 1993, Caligari et al. 1995).

In this paper we consider stars of $1 M_\odot$ in the early phases of their evolution (Hayashi phase until main sequence) and for rotation rates between $1\,\Omega_\odot$ and $60\,\Omega_\odot$. Both the field strength limit for undulatory instability and the relation between the forces that determine the trajectory of an erupting loop depend on the structure of the star and on its angular velocity. The critical field strength for instability is a complicated function of latitude, so that a detailed study of linear stability together with numerical simulations of the nonlinear evolution of the instability is necessary in order to assess the expected distribution of magnetic flux on the stellar surface.

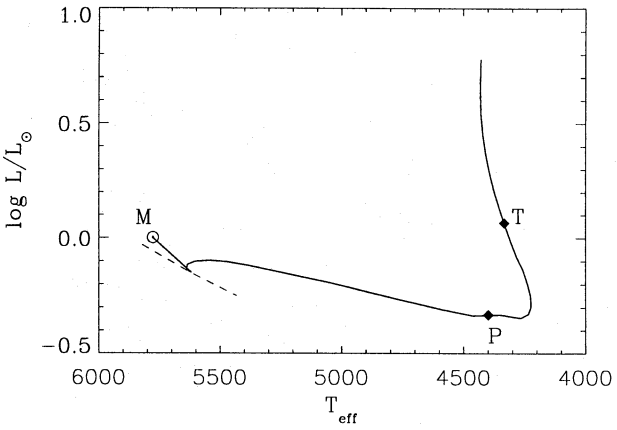

Fig. 1. Evolutionary path of a 1 $M_\odot$ star in the Hertzsprung-Russell diagram. The three models considered here are indicated. The corresponding part of the zero-age main sequence is denoted by the dashed line.

3. Stellar models and flux tube parameters

We consider stellar models from an evolutionary sequence for a star of 1 $M_\odot$ between the Hayashi track and the present Sun. The code used is based on the stellar evolution program originally developed by Kippenhahn et al. (1967) with modifications described by Stix & Skaley (1990). Most important for our purposes is the non-local description of the convective energy transport according to the method proposed by Shaviv & Salpeter (1973). This leads to a subadiabatically stratified overshoot layer below the outer convection zone of the stellar model, which is the assumed location for the generation and storage of magnetic flux tubes. The effect of rotation on the structure of the models is not included; even for $60\,\Omega_\odot$ the ratio of gravitational to centrifugal acceleration at the bottom of the convection zone is less than 5% for all models considered here.

The value of the mixing-length parameter, $\alpha = 2.4$, is determined together with the initial helium mass fraction, $Y_0 = 0.27$, by a calibration of the radius and the luminosity at the solar age with the observed values. α depends markedly on the opacity and, to a lesser degree, on the details of the equation of state. The large value of the present model results from the use of the Los Alamos Astrophysical Opacity Library (Weiss et al. 1990) and the equation of state in the analytical version described by

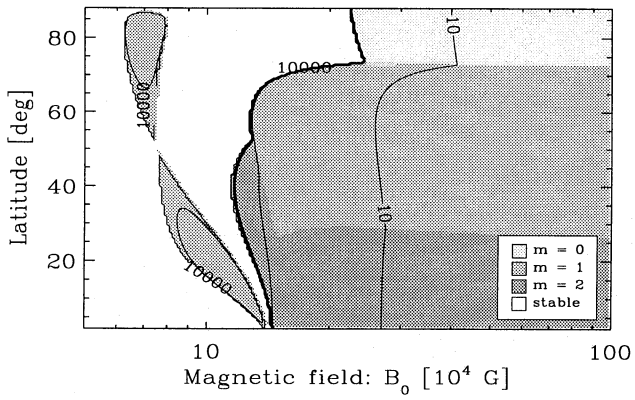

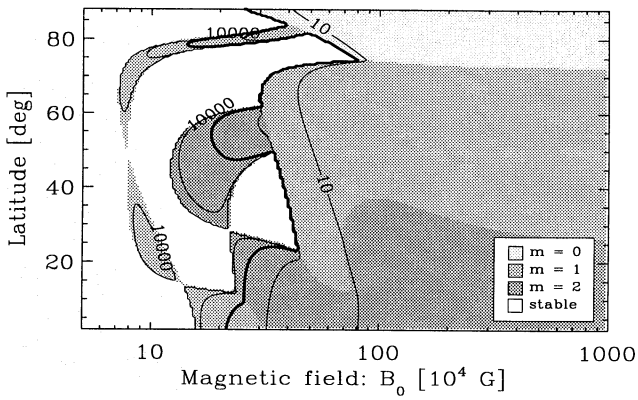

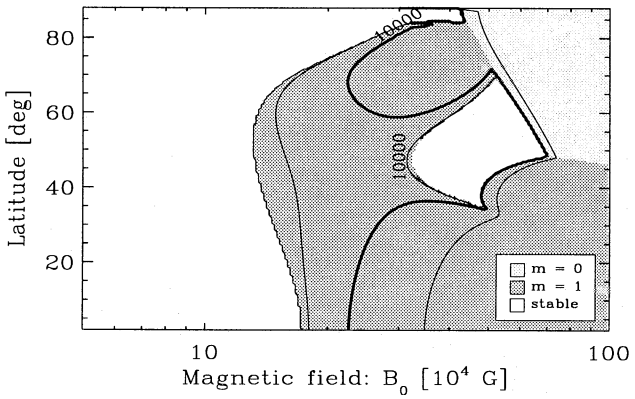

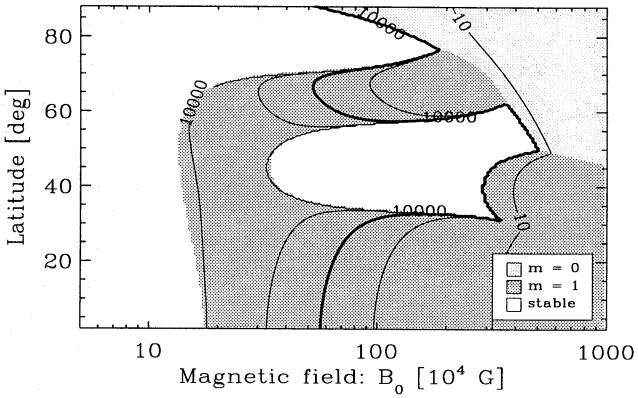

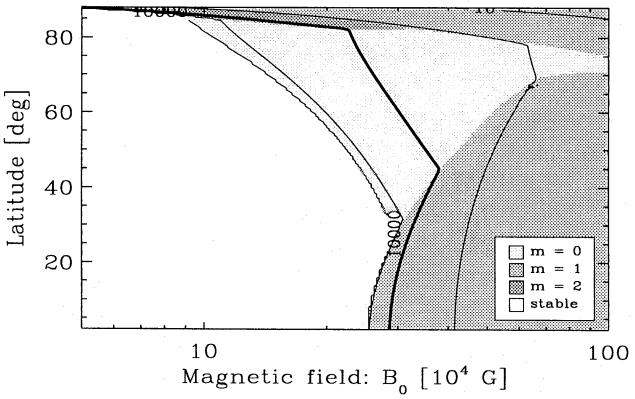

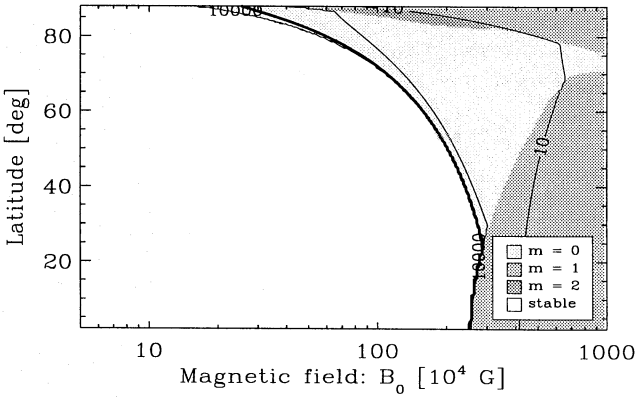

Fig. 2. Stability diagrams in the (B_0, λ_0) plane (B_0: field strength, λ_0: latitude of the equilibrium flux tube). White regions indicate stability, shaded regions instability. The degree of shading denotes the azimuthal wave number of the fastest-growing unstable mode. *top:* model M (Sun), *middle:* model P (pre-main-sequence star), *bottom:* model T (T Tauri star). Rigid rotation with the equatorial angular velocity of the Sun, $\Omega_\odot = 2.7 \cdot 10^{-6} \mathrm{s}^{-1}$, has been assumed.

Fig. 3. Same as Fig. 2, but for $\Omega = 10\,\Omega_\odot$. Note the change of scale on the horizontal axis. The main zone of instability has shifted to larger field strengths while the regions of weak instability (large growth time) for models M and P (top and middle panel) are almost unaffected. For these models an island-like region of stability between the zones of weak and strong instability has formed (model M), and grown (model P), respectively.

Stix & Skaley (1990). A model based on the OPAL opacity table (Rogers & Iglesias 1992) and on a MHD table for the equation of state (Mihalas et al. 1988) yields $\alpha = 1.68$. The structure of the convection zone in general remains almost unchanged in this model, although the overshoot layer is slightly shallower.

Fig. 1 gives the path in the Hertzsprung-Russell diagram corresponding to the calculated evolutionary sequence. The models considered here represent three distinct phases of this evolution: model 'T' on the lower part of the Hayashi track has already developed a small radiative core and may represent a T Tauri star; model 'P' is a pre-main-sequence star in the middle of its path from the Hayashi track onto the zero-age main sequence; finally, the Sun serves as a prototype main sequence star (model 'M'). Some properties of these models are listed in Table 1. Due

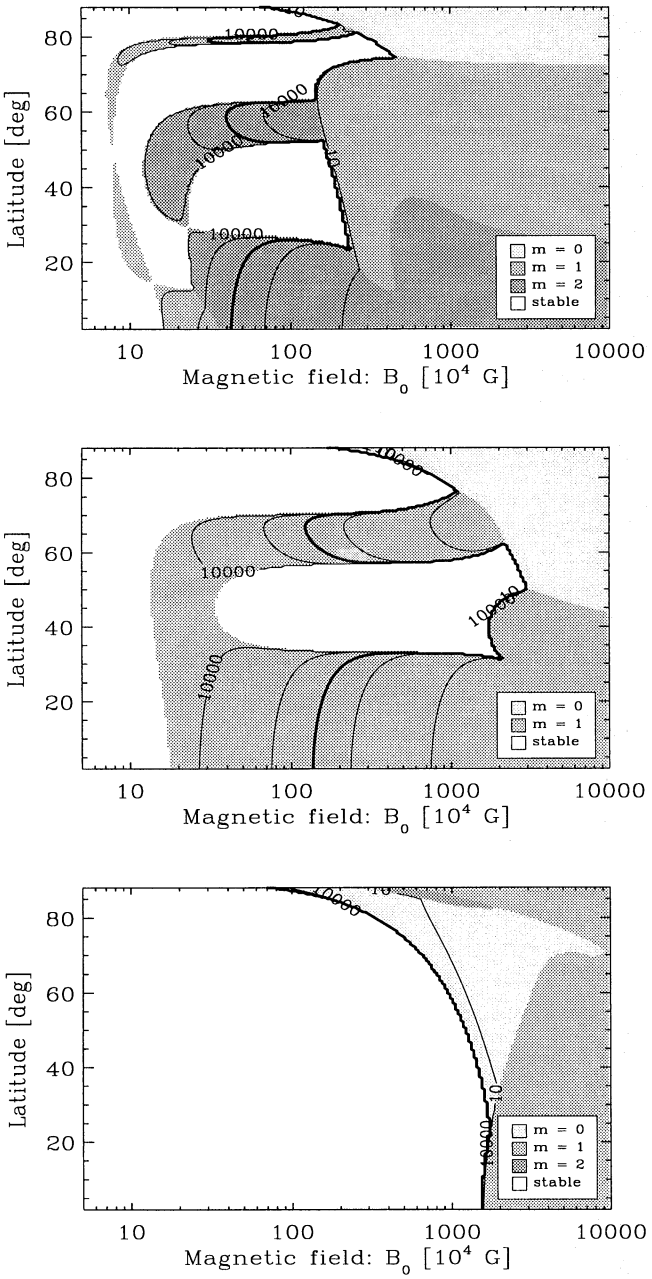

Fig. 4. Same as Fig. 3, but for $\Omega = 60\,\Omega_\odot$. Note that the scale on the horizontal axis has changed again. The stability islands for models M and P (top and middle panel) have grown strongly in comparison to Fig. 3; they now cover more than an order of magnitude in field strength. As a consequence, flux tubes becoming unstable at intermediate latitudes are dominated by the buoyancy force and rise almost radially (see Figs. 7 and 8).

to numerical difficulties, the non-local mixing length treatment does not yield useful results in the early phases of the evolution, including model T. We have therefore estimated the thickness of the overshoot layer and the superadiabaticity for this model using the formalism given by Zahn (1991). Comparison of such estimates with the actual values in the case of the other models leads to deviations of less than 30%, which seems acceptable given the uncertainties of any theoretical inference of the overshoot layer properties.

For each of the three stellar models we consider three values of the rotation rate, namely $1\,\Omega_\odot$, $10\,\Omega_\odot$, and $60\,\Omega_\odot$. This corresponds to rotation periods of about 27 days, 2.7 days, and 0.45 days, respectively. We assume rigid rotation in all cases. This seems justified since the differential rotation of the present Sun does not significantly influence the properties of rising flux loops (Caligari et al. 1995); for more rapidly rotating stars, an even smaller amount of differential rotation in the convection zone is indicated by observations (e.g., Hall 1990) and also predicted by theoretical models (e.g., Kitchatinov & Rüdiger 1995).

In accordance with the results of Caligari et al. (1995) for the Sun we assume that the flux tubes are stored near the bottom of the stellar overshoot layer, namely 2000 km above the transition to the radiative core. The value of 2000 km matches the radius of a flux tube with a field strength of 10^5 G containing 10^{22} Mx of magnetic flux, which corresponds to the observed flux of a large solar active region. The procedure to determine the emergence latitudes of erupting flux tubes is then as follows. In a first step we determine the stability properties of the stored flux tubes as a function of field strength and stellar latitude for a given stellar model and rotation rate. We then choose a value for the growth time of the undulatory instability and determine the corresponding field strength as a function of latitude. For these parameters we then perform the numerical simulation of the nonlinear development of the instability and follow the erupting loop(s) nearly up to the stellar surface until the thin flux tube approximation breaks down and the simulation has to be terminated. The equations and the numerical procedure underlying the simulation have been described by Caligari et al. (1995).

The relevant value of the growth time of the instability is related to the time scale of field amplification by the dynamo. We assume that the toroidal field is gradually amplified in a shear layer between stellar core and convective envelope. For some critical value of the field strength it becomes unstable. In most cases the growth time of the instability decreases with increasing field strength. As long as the the field strength remains so small that the growth time of the instability is much larger than the time scale of field amplification, the field strength can still increase during the slow development of the instability. Further amplification ceases when the growth time becomes comparable to the amplification time and the flux tube actually erupts. Consequently, the field strength of erupting flux tubes can be estimated by requiring the growth time of the instability to be of the order of the amplification time of the toroidal field in the shear layer. For the present Sun, a value of about one year for this time scale proved to be a reasonable choice (Caligari et al. 1995).

The amount of shear between core and envelope is not known for other stars, but we may tentatively take the observed latitudinal differential rotation on the surface as an indicator. Hall (1991) has studied the variation of the rotation rate, $\Delta\Omega$, over the range of spot latitudes for a large number of cool stars and found that $\Delta\Omega/\Omega \propto \Omega^{-0.8}$, i.e., the *relative* differential

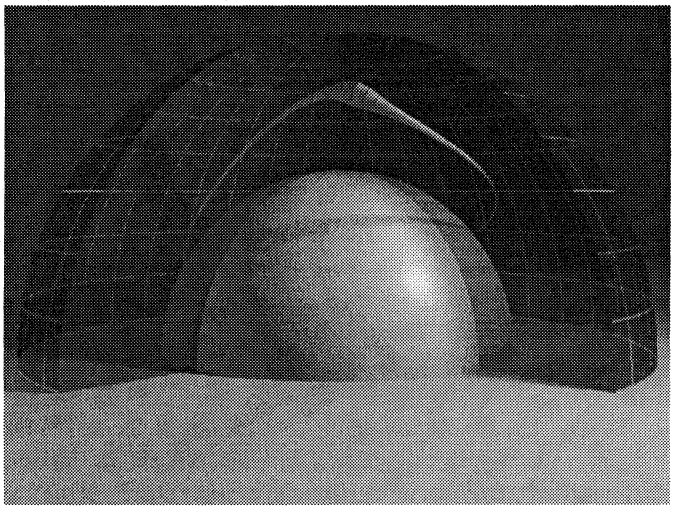

Fig. 5. Three-dimensional view of an unstable flux tube in model P, shortly before its eruption at the surface. The northern hemisphere of the star is represented; rotation ($\Omega = 10\Omega_\odot$) is counter-clockwise with respect to the vertical axis. The transparent outer half-sphere corresponds to the stellar surface while the inner half-sphere indicates the bottom of the convection zone.

Table 2. Values of density (ρ) and pressure scale height (H) in the overshoot regions of our three stellar models. The resulting factor that describes the influence of stellar structure on the minimum field strength for a significant effect of the buoyancy force on rising flux tubes according to Eq. 2 (Schüssler & Solanki 1992) is also given.

Model	ϱ [g·cm^{-3}]	H [cm]	$(H/H_\odot)(\varrho/\varrho_\odot)^{1/2}$
T	1.2	$3.9 \cdot 10^{10}$	18.5
P	1.6	$1.1 \cdot 10^{10}$	6.1
M	0.2	$5.7 \cdot 10^{9}$	1.0

rotation decreases for increasing angular velocity of the star. The amplification rate of of the toroidal field, however, is proportional to $\Delta\Omega$ itself, which is only weakly dependent on the rotation rate: $\Delta\Omega \propto \Omega^{0.2}$. We therefore conjecture that the time scales for stretching of the toroidal field are not drastically different for the stellar models considered here and assume a growth time of 300 days for most of our numerical simulations. Calculations with growth times of 100 and 500 days, respectively, have also been carried out in order to assess the dependence of the results on the choice of this parameter.

4. Stability diagrams

The stability properties of toroidal flux tubes stored in the convective overshoot layers of the stellar models M, P, and T for three values of the rotation rate are shown in Fig. 2 ($\Omega = \Omega_\odot$), Fig. 3 ($10\,\Omega_\odot$), and Fig. 4 ($60\,\Omega_\odot$). The individual panels give stability diagrams in the (B_0, λ_0)-plane, where B_0 is the field strength and λ_0 is the latitude of the equilibrium flux tube. In each figure the top panel corresponds to model M, the middle panel to model P, and the bottom panel to model T. Note that the horizontal scale (magnetic field) is not the same for the three figures. White regions in the stability diagrams denote stable flux tubes while the shaded regions indicate instability. The contour lines give the linear growth time of the instability; we give contours for 10000, 1000, 300, 100, and 10 days. The thick contour line in all diagrams corresponds to a growth time of 300 days. The degree of shading indicates the azimuthal wave number of the unstable mode with the largest growth rate. For $m \neq 0$ the instability leads to the formation of m rising flux loops which eventually emerge at the surface and form bipolar magnetic regions. The case $m = 0$ corresponds to the axisymmetric mode, i.e., the flux tube maintains the form of a toroidal flux ring during its rise. Presumably such a flux ring forms loops at some stage of its eruption, either due to nonlinear excitation of non-axisymmetric modes, local instability near the surface, or caused by the influence of convective velocities on the weakening flux tube.

A number of properties relevant to our problem can be derived from these diagrams:

1) Flux tubes with field strength significantly below 10^5 G are stable. Instability requires that a critical field strength is exceeded.
2) For model M (main-sequence star) and model P (pre-main-sequence star), instability sets in with small growth rates for field strengths of the order of 10^5 G. In the case of the T Tauri star (model T) field strengths up to 10^7 G (for $60\,\Omega_\odot$) are required for instability.
3) There is a 'main region' of instability extending to the right of the panels, for which the growth rate increases rapidly with B_0. This is the domain of the 'classical', buoyancy-driven Parker instability and probably constitutes the most relevant region for flux eruption. The region shifts towards larger field strength for increasing angular velocity and also for increasing depth of the convection zone (from model M to model T). The reason for this shift is the stabilizing influence of angular momentum conservation (increasing for growing angular velocity) and of magnetic tension (increasing for diminishing core radius).
4) Instability typically sets in for azimuthal wave numbers $m = 1$ or $m = 2$ for the buoyancy-driven modes. Axisymetric instabilities ($m = 0$), which are tension-driven, in most cases are restricted to the polar regions and large field strengths. For model T with its small core, however, the axisymmetric mode dominates down to low latitudes.
5) Model P, the pre-main-sequence star (and also model M for large rotation rate), shows an 'island of stability' at middle latitudes. This region expands towards larger field strength as the angular velocity increases. Growth rates to the left of the island are typically low, so that flux tubes stored in the corresponding latitude range probably erupt only at large field strength (to the right of the island).

The island of stability actually represents a stable transition between two different regimes of instability, one of which is only weakly dependent on rotation. As the other regime moves towards higher field strength for increasing angular velocity,

the transition region of stable flux tube equilibria (the island) widens.

As discussed in Sect. 3, we consider a growth time of about 300 days as relevant for the actual eruption of magnetic flux tubes. The stability diagrams show that in most cases the contour lines corresponding to these values are rather close to each other, so that we do not expect large differences in the nonlinear evolution of the instability. Comparing the different panels in the stability diagrams (Figs. 2-4) we find that the field strengths corresponding to 300 days growth time increase strongly with growing angular velocity. Consequently, both the buoyancy force and the Coriolis force grow as the rotation rate becomes larger, so that we cannot say beforehand whether increasing the rotation rate necessarily leads to a strong poleward deflection. This question has to be answered by following the trajectories of rising flux tubes during the nonlinear development of the instability.

5. Surface distribution of emerging flux

We follow the nonlinear evolution of the instability by a numerical simulation. The simulation code is based on the thin flux tube approximation (for details see Moreno-Insertis 1986; Caligari et al. 1995). We start from a flux ring in equilibrium and perturb it with a superposition of sinusoidal displacements with azimuthal wave numbers in the range $m = 1 \ldots 5$. If the fastest growing mode has $m \neq 0$ rising loops form, traverse the convection zone and finally erupt at the surface, while the remaining part of the flux tube sinks towards the bottom of the overshoot layer and becomes 'anchored'. We cannot simulate the actual eruption process at the surface and the subsequent evolution since the thin flux tube approximation breaks down when the flux tube expands rapidly as it approaches the surface.

As an example, Fig. 5 gives a three-dimensional view of the final state of such a simulation. The corresponding equilibrium flux tube was located in the overshoot layer of the pre-main-sequence star (model P) at a latitude of 15 deg. The assumed rotation rate is $10\,\Omega_\odot$. The outer (transparent) half-sphere corresponds to the stellar surface while the inner (opaque) half-sphere indicates the bottom of the convection zone. The dominant mode of the instability is $m = 1$, so that one loop has formed and risen through the convection zone. The decreasing external gas pressure leads to a strong expansion of the upper part of the erupting loop, which is easily visible as a 'bulge'. Obviously, the effect of the Coriolis force dominates the dynamics in this case, so that the rising loop has been strongly deflected poleward to emerge at a latitude of 50 deg. The remaining part of the flux tube is anchored at the bottom of the overshoot layer, nearly at its initial latitude of 15 deg.

We have performed a number of simulation series. For a given stellar model (M, P, or T) and a given rotation rate (1, 10, $60\,\Omega_\odot$) we consider initial flux rings located 2000 km above the bottom of the respective overshoot layer and at latitudes between 5° and 60°. Their initial field strength is determined by following a contour line of constant growth time in the corresponding stability diagram (Figs. 2-4). In most cases we have assumed a growth time of 300 days and a magnetic flux of 10^{22} Mx; cases with growth times of 100 days and 500 days have also been considered in order to assess the influence of this parameter.

Since we are mainly interested in the amount of poleward deflection and in the emergence latitudes, it is sufficient to study the trajectories of the rising loop summits in a meridional projection. Figs. 6-8 show the results for the different models and values of the stellar angular velocity considered here. Only in the case of the present Sun (model M, $\Omega = \Omega_\odot$, top panel of Fig. 6) we find an almost radial rise of the emerging flux loops. All other cases show a significant poleward deflection up to nearly axis-parallel rise (model T, bottom panel of Fig. 6); observationally, such stars would show at least an 'equatorial gap' in their surface distribution of magnetic features.

The range of latitudes over which magnetic flux emerges at the stellar surface depends on the rotation rate as well as on the stratification and depth of the stellar convection zone. For increasing rotation rate the mean latitude of emergence shifts poleward since the Coriolis force increasingly gains influence on the dynamical evolution of the rising magnetic flux loops. By comparing Figs. 7 and 8 we recognize that in most cases the Coriolis force dominates the evolution of the flux tube already for $\Omega = 10\,\Omega_\odot$; increasing the rotation rate to $60\,\Omega_\odot$ does not lead to a further significant change of the trajectories.

On the other hand, for the models of young stars (T, P) we find a strong poleward deflection even for a rotation rate as low as $\Omega_\odot$ (see Fig. 6). These stars have deeper convection zones than model M and also the superadiabaticity in the main part of their convection zones is about an order of magnitude smaller than for the solar model. This leads to longer rise times of magnetic loops and weakens the driving of the rise by convective buoyancy during the nonlinear development of the Parker instability. Both effects favor the dominance of the Coriolis force and lead to much stronger poleward deflection than in the case of the Sun.

For the T Tauri star (model T) the axisymmetric mode ($m = 0$) is dominant in the linear phase of the instability, so that the influence of angular momentum conservation and Coriolis force is particularly strong. Moreover, model T has a much larger scale height near the bottom of its convection zone than the other models; this leads to a weaker buoyancy force and so favors the dominance of the Coriolis force. In the calculations performed for the bottom panel of Figs. 6 we have assumed that the flux tubes remain axisymmetric during their whole evolution. In reality, however, non-axisymmetric modes will be excited nonlinearly, loops form and eventually bipolar magnetic regions emerge at the surface.

The bottom panels of Figs. 7 and 8 show cases with 500 days and 100 days growth time, respectively. Both are for model P and should be compared with the panels directly above them, which give the same cases for 300 days growth time. The somewhat smaller (larger) field strength compared to the middle panel of Fig. 7 (Fig. 8) leads to a somewhat stronger (weaker) poleward deflection. The effect is rather small, however, so that we may conclude that the precise choice of the growth time has no significant influence on our results unless extreme values are taken.

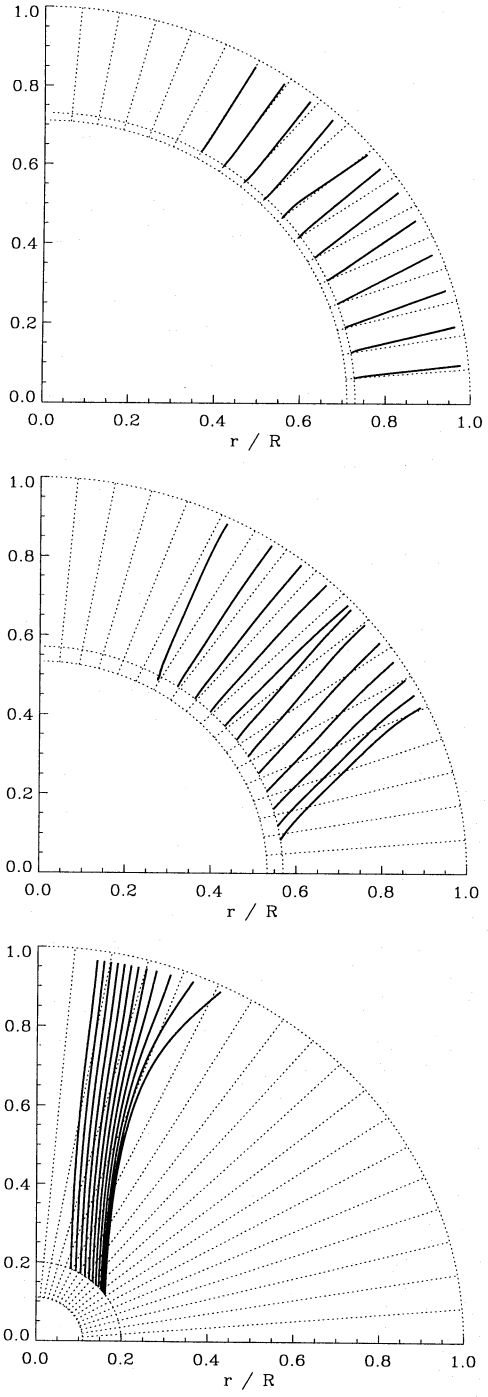

Fig. 6. Trajectories of the crests of the rising flux tubes in a meridional projection. The location of the overshoot layer and the radial direction are marked by dotted lines. *top:* model M (main-sequence star), *middle:* model P (pre-main-sequence star), *bottom:* model T (T Tauri star). Rigid rotation with the equatorial angular velocity of the present Sun, $\Omega_\odot = 2.7 \cdot 10^{-6} \mathrm{s}^{-1}$, has been assumed. In all the plotted cases, the trajectories start when the summit of the rising loop has left the overshoot layer.

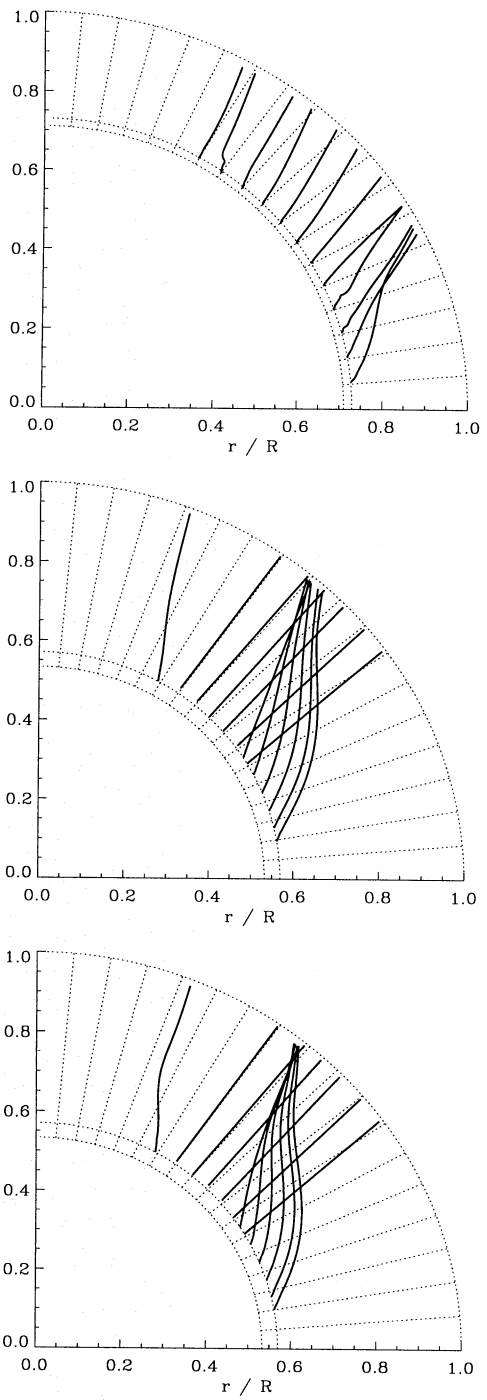

Fig. 7. Trajectories of the crests of the rising flux tubes for $\Omega = 10\,\Omega_\odot$. *top:* model M (main-sequence star), *middle:* model P (pre-main-sequence star), *bottom:* model P, but for 500 days growth time of the instability. The larger rotation rate leads to a stronger poleward deflection of the trajectories as compared to Fig. 6.

It is of some interest to compare the detailed results shown above to the estimates of the minimum field strength, $B_{\min}$, for a significant influence of the buoyancy force (and, therefore, radial eruption) given by Schüssler & Solanki (1992; see their Eqs. 7 and 8). In terms of the solar values for the scale height, $H_\odot = 5.7 \cdot 10^9$ cm, and density, $\rho_\odot = 0.2$ g·cm^{-3}, in the overshoot we have

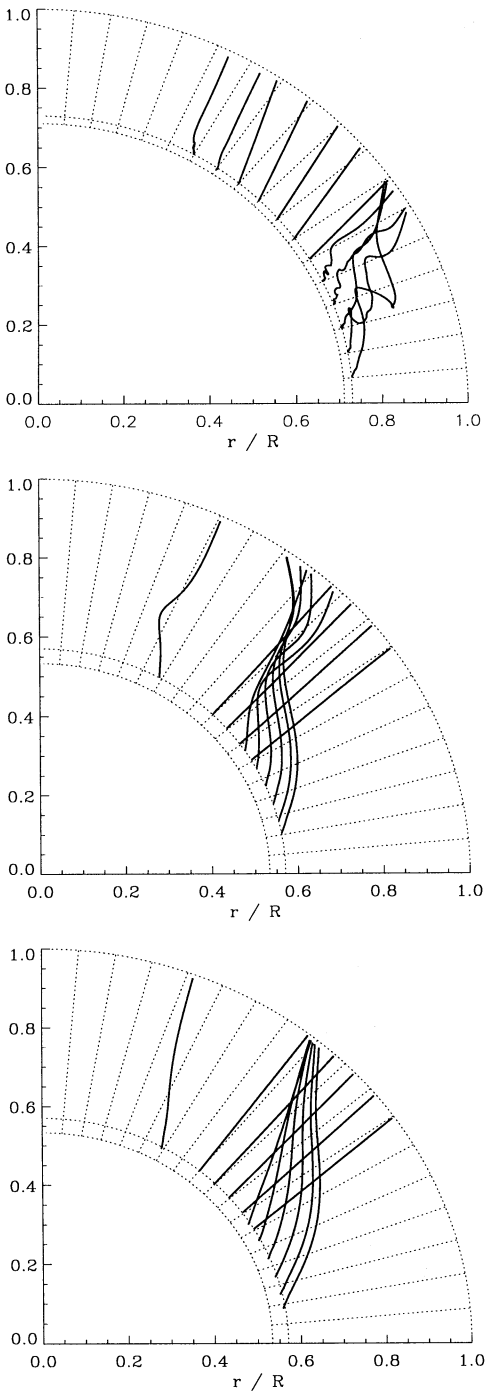

Fig. 8. Trajectories of the crests of the rising flux tubes for $\Omega = 60\,\Omega_\odot$. *top:* model M (main-sequence star), *middle:* model P (pre-main-sequence star), *bottom:* model P, but for 100 days growth of the instability. Large-amplitude waves due to the rapid rotation cause difficulties for the routine that determines the loop summit in some cases of the top panel. This leads to the seemingly irregular trajectories; the actual evolution of the flux loop, however, is much smoother.

$$B_{\rm min} \simeq 10^5 \left(\frac{H}{H_\odot}\right) \left(\frac{\varrho}{\varrho_\odot}\right)^{1/2} \left(\frac{\Omega}{\Omega_\odot}\right) \,{\rm G}\,. \qquad (2)$$

Tab. 2 gives the values of density and scale height for the stellar models considered here, together with the resulting factors in Eq. (2). We see that, for a given rotation rate, flux tubes in young stars of one solar mass should be much more influenced by the Coriolis force than in the case of a main-sequence star. The physical reason is the larger scale height, which diminishes the buoyancy force, and the larger density, which increases the rise time. From inspection of the corresponding stability diagrams in Figs. 2-4 we find that the present Sun (model M, $\Omega = \Omega_\odot$) is the only case for which instability with significant growth rate (growth time < 500 days) sets in for field strengths *above* the corresponding value resulting from Eq. (2). In all other cases, the criterion of Schüssler & Solanki (1992) predicts significant poleward deflection, which is in full agreement with the numerical results given in Figs. 6-8.

Apart from the Sun, the only other exception from rotation-dominated rise in our sample is related to the island-like region of stable flux tubes in the stability diagrams for the models M and P. While for $\Omega = \Omega_\odot$ significant growth rates are reached on the *left-hand* side of the island (low field strength), for the larger values of the rotation rate the contour lines for a relevant growth of the instability bend towards the *right-hand* side of the island, which corresponds to much larger field strengths of the erupting loops. From the middle panels of Figs. 3 and 4 we see that the field strength of flux tubes stored at intermediate latitudes in model P has to be about one order of magnitude larger than in low latitudes in order to reach a growth time of 300 days. As can be seen in the middle panels of Figs. 7 and 8, the buoyancy force dominates the rise in these cases and leads to nearly radial trajectories of the flux loops, in spite of the large rotation rate. Therefore, we may expect magnetic flux emergence in the latitude range of the stability island, irrespective of the rotation rate of the star. This result could well be related to the starspots observed at intermediate latitudes of rapidly rotating pre-main-sequence stars.

6. Conclusion

We have shown that the observed latitude distribution of magnetic features on young stars of about one solar mass can be understood as a consequence of the interplay between buoyancy force and Coriolis force acting on rising flux tubes. The buoyancy force depends mainly on the magnetic field strength of the tube and on the superadiabaticity of the stratification of the stellar convection zone, while the Coriolis force is directly proportional to the rotation rate of the star.

Models of young stars which have not yet reached the main sequence have such deep convection zones and small superadiabaticity that the Coriolis force dominates even for the slow rotation rate of the present Sun and leads to a significant poleward deflection of the rising flux tubes. Observationally, these stars would show a pronounced equatorial gap in their surface distribution of magnetic features (pre-main-sequence stars) or even a magnetic coverage of the polar cap (T Tauri stars). For a given stellar model, increasing rotation rate leads to a poleward

shift of the latitude range of magnetic flux emergence. However, the stability properties in the middle latitudes (between 30° and 60°, say) of pre-main-sequence and main-sequence stars are such that only flux tubes with very strong field form rising flux loops; these loops rise more or less radially and lead to magnetic features at intermediate latitudes, independent of the rotation rate of the star. Hence, the simultaneous existence of high-latitude starspots and magnetic features at middle latitudes of young rapid rotators can be understood as a consequence of the stability properties of toroidal flux rings, together with the dynamics of rising flux loops.

Since our simulations do not include the actual flux emergence at the stellar surface and the subsequent evolution of the magnetic structures we cannot take into account the potential effect of meridional circulation on the latitude distribution of starspots. In the case of the Sun, a poleward surface flow may be important for the evolution of non-spot magnetic fields within the solar cycle (e.g., Dikpati & Choudhuri 1994), but there does not seem to be a significant effect on sunspots. Surface flows as well as the dynamical evolution of the underlying magnetic loop after flux emergence remain to be investigated in detail. Preliminary calculations show that for very strong field (as in the 'island' cases) and for a sufficiently small stellar core the force equilibrium of the 'anchored' part, which is described by Eq. (1), breaks down when a loop erupts: angular momentum conservation in the rising loop decelerates the equilibrium flow along the tube and the tension force is no longer balanced. As a result, the anchored part slips towards the pole like a rubberband on a polished sphere and pulls the emerged loop poleward as well. This process opens an alternative path for the evolution of polar spots: magnetic flux emerges in mid latitudes and then migrates to the poles to supply the magnetic polar cap. In this way, the simultaneous existence of truly polar spots and mid-latitude features could possibly be understood.

In summary, our results indicate that the concept of storage, instability and nonlinear rise of magnetic structures (Schüssler et al. 1994), which has been successfully applied to understand the properties of solar magnetic active regions, is equally useful for evolving young stars over a broad range of rotation rates. A subsequent paper will be concerned with the dynamics of magnetic structures in more evolved stars (subgiants and giants).

References

Caligari, P., Moreno-Insertis, F., Schüssler, M. 1995, ApJ 441, 886
Cattaneo, F., Hughes, D.W. 1988 J. Fluid Mech. 196, 323
Choudhuri, A.R., Gilman, P.A. 1987, , ApJ 316, 788
Collier Cameron, A., Unruh, Y.C. 1994, MNRAS 269, 814
Dikpati, M., Choudhuri, A.R. 1994, A&A 291, 975
Donati, J.-F., Brown, S.F., Semel, M. et al., 1992, A&A 265, 682
D'Silva, S., Choudhuri, A.R. 1993, A&A 272, 621
Ferriz-Mas, A., Schüssler, M. 1993, Geophys. Astrophys. Fluid Dyn. 72, 209
Ferriz-Mas, A., Schüssler, M. 1994, ApJ 433, 852
Ferriz-Mas, A., Schüssler, M. 1995, Geophys. Astrophys. Fluid Dyn. 81, 233
Hall, D.S. 1990, in The Sun and Cool Stars: Activity, Magnetism, Dynamos, I. Tuominen, D. Moss, G. Rüdiger (Eds.), Springer, Heidelberg, IAU Coll. 130, p. 353
Hatzes, A.P. 1995, ApJ 451, 784
Hatzes, A.P., Vogt S.S. 1992, MNRAS 258, 387
Jankov, S., Char, S., Foing, B.H. 1992, in Solar Physics and Astrophysics at Interferometric Resolution, L. Damé, T.D. Guyenne (Eds.), ESA, SP-344, p. 113
Joncour, I., Bertout, C., Ménard, F. 1994a, A&A 285, L25
Joncour, I., Bertout, C., Bouvier, J. 1994b, A&A 291, L19
Kippenhahn, R., Weigert, A., Hoffmeister, E. 1967, Meth. Comp. Phys., 7, 129
Kitchatinov, L.L., Rüdiger, G. 1995, A&A 299, 446
Kürster, M., Hatzes, A.P., Pallavicini, R., Randich, S. 1992, in Seventh Cambridge Workshop on Cool Stars, Stellar Systems, and the Sun, M.S. Giampapa, J.A. Bookbinder (Eds.), ASP Conf. Series, Vol. 26, p. 249
Kürster, M., Schmitt, J.H.M.M., Cutispoto, G. 1994, A&A 289, 899
Mihalas, D., Däppen, W., Hummer, D.G. 1988, ApJ 331, 815
Moreno-Insertis, F., Schüssler, M., Ferriz-Mas, A. 1992, A&A 264, 686
Moreno-Insertis, F., Caligari, P., Schüssler, M. 1994a, in Solar Surface Magnetism, R.J. Rutten, C.J. Schrijver (Eds.), Kluwer, Dordrecht, 407
Moreno-Insertis, F., Caligari, P., Schüssler, M. 1994b, Sol. Phys. 153, 449
Parker, E.N. 1975, ApJ 198, 205
Proctor, M.R.E., Weiss, N.O. 1982, Rep. Progr. Phys. 45, 1317
Rogers, F.J., Iglesias, C.A., 1992, ApJSS 79, 507
Saar, S.H., Piskunov, N.E., Tuominen, I. 1994, in Cool Stars, Stellar Systems, and the Sun, VIII, J.-P. Caillault (Eds.), Astron. Soc. Pacific Conf. Ser. Vol. 64, p. 661
Schüssler, M., Solanki, S.K. 1992, A&A 264, L13
Schüssler, M., Caligari, P., Ferriz-Mas, A., Moreno-Insertis, F. 1994, A&A 281, L69
Shaviv, G., Salpeter, E.E. 1973, ApJ 184, 191
Spiegel E.A., Weiss N.O. 1980, Nature 287, 616
Spruit, H.C. 1981, A&A 102, 129
Spruit, H.C., van Ballegooijen, A.A. 1982, A&A 106, 58
Stix, M., Skaley, D. 1990, A&A 232, 234
Strassmeier, K.G. 1990, ApJ 348, 682
Strassmeier, K.G. 1994, A&A 281, 395
Strassmeier, K.G., Rice, J.B., Wehlau, W.H. et al., 1991, A&A 247, 130
Strassmeier, K.G., Welty, A.D., Rice, J.B. 1994, A&A 285, L17
Unruh, Y.C., Collier Cameron, A., Cutispoto, G. 1995, MNRAS 277, 1145
Vogt, S.S. 1988, in The Impact of Very High S/N Spectroscopy on Stellar Physics, G. Cayrel de Strobel, M. Spite (Eds.), Kluwer, Dordrecht, IAU Symp. 132, 253
Vogt, S.S., Hatzes, A.P. 1991, in The Sun and Cool Stars: Activity, Magnetism, Dynamos, I. Tuominen, D. Moss, G. Rüdiger (Eds.), Springer, Berlin, p. 297
Vogt, S.S., Penrod, G.D. 1983, PASP 95, 565
Weiss, A., Keady, J.J., Magee, Jr.,N.H. 1990, Atomic Data and Nuclear Data Tables, 45, 209
Zahn, J.P. 1991, A&A 252, 179
Zwaan, C., Harvey, K.L. 1994, in Solar Magnetic Fields, M. Schüssler & W. Schmidt (Eds.), Cambridge University Press, Cambridge/UK, p. 27